GMR
The Original

GREEN SYNTHESIS OF *JUGLANS REGIA*-MEDIATED GOLD NANOPARTICLES CONJUGATED WITH 5-FLUOROURACIL: CHARACTERIZATION AND *IN VITRO* ANTICANCER ACTIVITY AGAINST MCF-7 BREAST CANCER CELLS.

E. V. Sheena[1*], A. K. Rathna Kumari[2], L. Monisha[3]

[1*]PG Department of Plant Biology and Plant Biotechnology, Shrimathi Devkunvar Nanalal Bhatt Vaishnav College for Women, Chrompet, 600044, Tamil Nadu. India, Email: sheenasdnbvc@gmail.com
[2,3]PG Department of Plant Biology and Plant Biotechnology, Shrimathi Devkunvar Nanalal Bhatt Vaishnav College for Women, Chrompet, 600044, Tamil Nadu. India

ABSTRACT

Juglans regia-L. (Juglandaceae), commonly known as walnut, is an important medicinal plant known for its diverse phytochemical constituents and potential biological activities. The present study aimed to investigate the preliminary phytochemical composition of *Juglans regia*-extract using qualitative phytochemical screening methods. The analysis revealed the presence of saponins, whereas alkaloids, carbohydrates, glycosides, proteins and amino acids, phenolic compounds, flavonoids, terpenoids, and steroids were not detected under the experimental conditions. Green synthesis of gold nanoparticles (AuNPs) was carried out using the aqueous extract of *Juglans regia*, which acted as both a reducing and capping agent. The formation of AuNPs was confirmed through various characterization techniques, including UV–Vis spectroscopy, EDAX and XRD analysis. The findings showed that *Juglans regia*-mediated AuNPs possess IC_{50} of 79.12 % against MCF-7 cells. Hence, from the study *Juglans regia*-mediated AuNPs demonstrated promising anticancer potential, with concentration-dependent cytotoxic effects against MCF-7 breast cancer cells. Their bioactivity suggests potential for further investigation as a candidate for cancer-related nano biomedical applications.

KEYWORDS: *Juglans regia*, Phytochemicals, AuNPs, MCF-7 cells, Green synthesis

Graphical Abstract

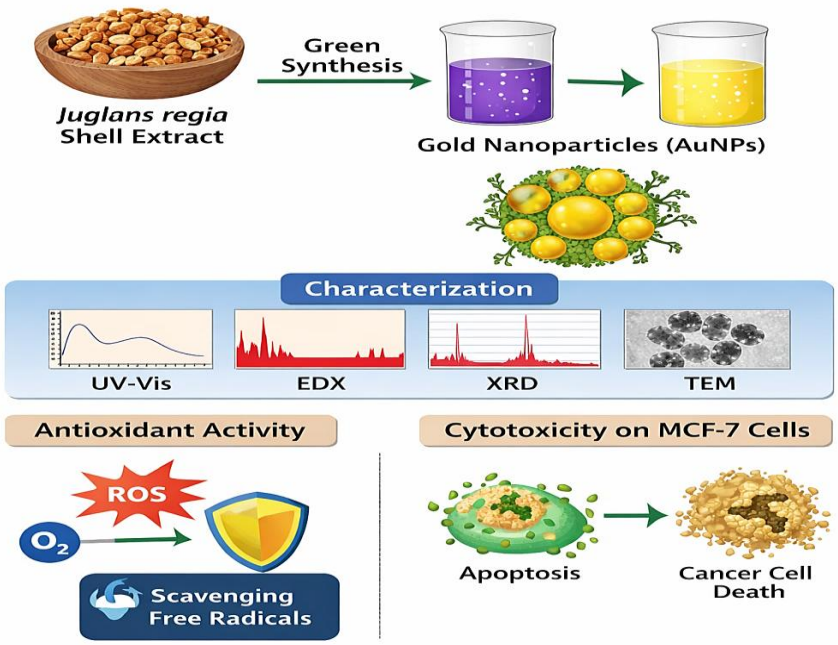

INTRODUCTION

Green synthesis is an eco-friendly, sustainable approach for producing nanoparticles and other valuable materials using biological systems instead of hazardous chemical methods. Among various biological routes, plant-mediated synthesis has gained significant attention due to its simplicity, cost-effectiveness, and environmental compatibility (1).

Plant extracts contain a wide range of bioactive compounds such as flavonoids, alkaloids, phenolics, terpenoids, proteins, and sugars. These phytochemicals act as natural reducing, stabilizing, and capping agents during the synthesis process.

When plant extracts are mixed with metal salt solutions (e.g., silver nitrate or chloroauric acid), the biomolecules reduce metal ions into nanoparticles while simultaneously preventing aggregation, resulting in stable nanomaterials (2).
Compared to conventional physical and chemical synthesis methods—which often require high temperature, high pressure, and toxic chemicals—plant-based green synthesis operates under mild conditions and minimizes environmental impact. This method aligns with the principles of green chemistry, including waste prevention, safer solvents, renewable feedstocks, and energy efficiency.
Green synthesis using plants has been widely applied in the production of silver, gold, zinc oxide, and copper nanoparticles. These biogenic nanoparticles exhibit promising applications in antimicrobial activity, drug delivery, catalysis, environmental remediation, and biomedical fields. Due to its sustainability, scalability, and reduced toxicity, plant-mediated green synthesis is emerging as a powerful alternative to traditional nanomaterial fabrication techniques and plays a crucial role in advancing environmentally responsible nanotechnology (3,4).
Gold nanoparticles synthesized from plant extracts have been widely investigated for targeted drug delivery and photothermal therapy, whereas silver nanoparticles show strong cytotoxic and anti-proliferative activity against various cancer cell lines, including breast, lung, colon, and cervical cancers. The synergistic effect of phytochemicals present on the nanoparticle surface further enhances their therapeutic potential by contributing intrinsic anticancer activity (5).

METHODOLOGY

Phytochemical Analysis

Phytochemical analysis of the extracts of different plants was carried out using standard protocols [6-9].

Antioxidant activities

The antioxidant potential of the AuNPs was determined by DPPH free radical scavenging assays. The DPPH free radical scavenging potential of synthesized AuNPs was examined according to a standard procedure [10]. Briefly, aliquots (1.6 mL) of various concentrations of AuNPs (20–150 lg/mL) in Milli-Q water were added to0.4 mL of 0.1 mM DPPH in methanol. The reaction mixture was mixed properly and incubated in the dark at 37˚C at selected durations up to 30 min while shaking at 100 rpm Absorbance was read against a blank at 517 nm using a UV– vis spectrophotometer. The percentage inhibition of DPPH oxidation was calculated using the following equation:
%Inhibition = (A blank / A sample) = A blank x 100
Where A blank is the absorbance value of the control and A sample is the absorbance value of the test sample. Ascorbic acid was used as a reference and tests were conducted in triplicate.

Preparation of gold nanoparticles

5FU and gold nanoparticles conjugate was prepared by adding, 0.5g of PEG and add 3ml of AuNPs to stirred for 2 hours and add 5µg/ 5-FU of the synthesized gold nanoparticles and it was stirred effectively in the rotary shaker at 8000 rpm 20min for 4-6 hrs and pH was 7.0 to enhance the interaction between 5-FU and gold nanoparticles [11].
Biosynthesis of gold nanoparticles was carried out using the aqueous extract shells of each shell samples were taken and added to 9.0 ml of 1.0 M mol of HAuCl4. The reaction was incubated at room temperature in dark condition for 24 hrs and observed for any change in color. The formation of ruby red color confirms the synthesis of AuNPs. The confirmation of color change was done by analyzing the absorption peak over the range of wavelength from 300 nm to 700 nm. The biological reduction of chloro aurate was recorded under UV-visible spectroscopy using PC based systolic double beam spectrophotometer 2202.

Cell Culture Maintenance

VERO African green monkey kidney normal cell line and MCF-7 human breast epithelial adenocarcinoma cancer cell line were obtained from the National Centre for Cell Sciences (NCCS), Pune, India. Cells were maintained in the logarithmic phase of growth in Dulbecco's modified eagle medium (DMEM) supplemented with 10% (v/v) heat inactivated fetal bovine serum (FBS), 100 U/mL penicillin, 100 µg/mL streptomycin. They were maintained at 37°C with 5% CO2 in 95% air humidified incubator.

Cytotoxicity effect on cell lines

The Cytotoxicity effect of the sample was tested against VERO and MCF-7cell lines by MTT (3-(4,5-dimethylthiazol-2-yl)-2,5-diphenyltetrazolium bromide assay (Mossman, 1983). The cells were seeded in 96-well micro plates (1 x 106 cells/well) and incubated at 37°C for 48 h in 5% CO2 incubator and allowed to grow 70-80% confluence. Then the medium was replaced and the cells were treated with different concentrations (25, 50, 75, 100, 125 µg/mL) of sample and incubated for 24 h. The morphological changes of untreated (control) and the treated cells were observed under inverted microscope (20Xmagnification) after 24 h and photographed. The cells were then washed with phosphate-buffer saline (PBS, pH-7.4) and 20 µL of (MTT) solution (5 mg/mL in PBS) was added to each well. The plates were then stand at 37ºC in the dark for 2h. The formazan crystals were dissolved in 100 µL DMSO and the absorbance was read spectrometrically at 570nm. Percentage of cell viability was calculated using the formula,
Cell viability (%) = (Absorbance of sample/Absorbance of control) X 100.
Graph was plotted using the cell viability (%) at Y-axis and concentration of the sample in X-axis. The concentration that inhibited 50% of cell growth referred to as IC50 value was determined [12].

Transmission electron microscopy (TEM)
In order to study the localization of AuNPs after activating in the cell, transmission electron microscopy (TEM) was performed with the same specimens as being used for microscopy. The TEM data indicated preferred arrangements of AuNPs between the membranous structures and the cell nucleus which could be assigned to be endoplasmic reticulum.
Energy dispersive X-ray spectroscopy (EDX)
A drop of AuNPs was placed on aluminum foil and allowed to stand for 2 min, and the excess solution was removed using a blotting paper allowed to dry at 50°C. EDX analyses of different elements were recorded with the above instrument.

X-ray diffraction (XRD)
The crystalline nature of the gold nanoparticles was revealed by XRD analysis. The gold nanoparticles were placed on a glass disk (~5 mm diameter) for drying and then mounted in the specimen port of the diffract meter. The XRD pattern was observed with Cu Kα radiation with the operating condition at 40 kV, 100 mA and scanned in the 2θ range from 20° to 80° with step size 0.02° per second.

Fourier transforms infrared spectroscopy (FTIR)
The formation of AuNPs and its stabilizing bimolecular were analyzed using FTIR (Perkin–Elmer spectrum). All measurements were carried out in the range of 500–4000 cm−1 at a resolution of 4 cm−1. The biomolecule that is present in the extract which was responsible for capping was identified. The various modes of vibrations were identified and assigned to determine the different functional groups present in the sample [13].

RESULTS
Extract preparation
100g of shells of *Juglans regia*-was washed under running tap water to remove the debris. To the sample 500 mL sterile water was added and extracted using hot continuous soxhlet extraction method to obtain the extract. After cooling, the extract was filtered and stored in amber bottle at 4°C for further analysis (Fig.1,2).

Fig. 1. Fruit and shell powder of *J. regia*

Fig. 2. Aqueous extract of *J. regia*

Phytochemical Analysis
Among the phytoconstituents tested, the nanoparticles synthesized shell extract of *Juglans regia*-showed the presence of saponins which is represented in the table 1. Studies have indicated that *Juglans regia*-shells and husks contain significant levels of bioactive compounds, including saponins, which contribute to their medicinal properties [14,15]. Additionally, a study has outlined standard phytochemical screening methods confirming saponins in plant extracts, supporting the reliability of such findings [16].

Table 1: Phytochemical screening of aqueous extract of AuNPs *Juglans regia*

Phytocomponents	Inference
Alkaloids	-
Carbohydrates	-
Glycoside	-
Saponin	+
Protein and Aminoacids	-
Aminoacids	-
Phenolic compound	-

Flavonoid compound	-
Terpenoid	-
Steroids	-

Nanoparticles Synthesized

The reduction of HAuCl4 and synthesis of gold nano particles from the aqueous extract of the shells of *Juglans regia*-was confirmed by the formation of ruby red color. The absorption peak was recorded at 532 nm for the extract (Fig. 3). The interaction of gold nanoparticles with biomolecules of aqueous shell extract of *J. regia* was inferred by UV analysis. The UV spectra showed a sharp peak at 532nm (Fig. 3). Similar studies observed characteristic absorption peaks at 530–537 nm with corresponding ruby-red to purple color changes when $HAuCl_4$ was reduced by other plant extracts, supporting the validity of this approach for eco-friendly nanoparticle synthesis (e.g., *Ziziphus ziziphus* leaf extract showing SPR ~537 nm) [17].

Fig. 3

AuNPs synthesized from aqueous extract of *J. regia*

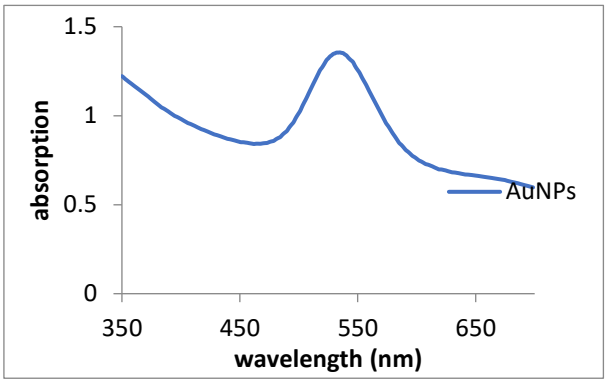

UV of AuNPs synthesized from aqueous extract of *J. regia*

Effect of pH

The stability of synthesized AuNPs tested in different pH was recorded at 37° C. The absorbance of solution is measured between 300-700nm using spectrophotometer after 24hrs. Highest stability was observed at pH 7 (Fig. 4, Table 2). This observation is consistent with previous reports demonstrating that AuNPs often exhibit enhanced stability near neutral or physiological pH, where the electrostatic repulsion and optimal capping agent interaction prevent agglomeration, whereas extreme acidic or alkaline environments tend to destabilize nanoparticles by disrupting surface capping and altering surface charge. Such pH-dependent behavior underscores the importance of optimizing synthesis and storage conditions for biomedical applications where neutral pH is predominant [18].

Table 2: Effect of pH of aqueous extract of AuNPs *Juglans regia*

pH value	**Nanometer**
pH 3	546.0
pH 5	551.4
pH 7	551.6
pH 9	540.4
pH 11	529.2

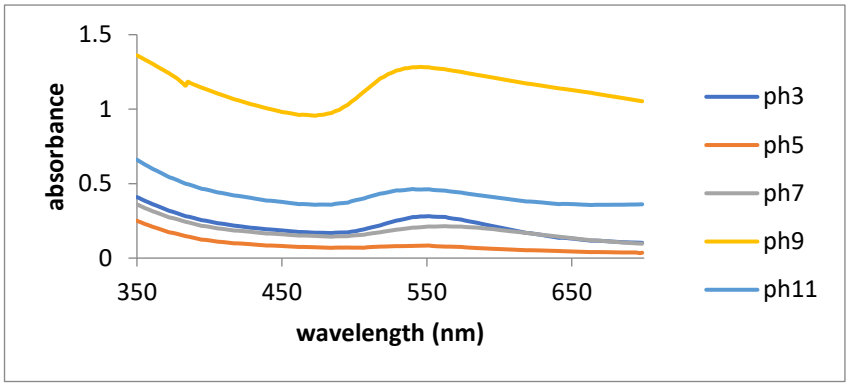

Fig. 4. Effect of pH of AuNPs synthesized from aqueous extract of *J. regia*

Temperature

Effects of different temperature are considered as1.0ml of shell extract and add 9.0ml of 1mm HAuCL4 add (pH 7.0). Incubated at different temperature as 12°C, 22°C, 37°C, 48°C, 60°C, for 24 hrs. Effect of temperature shown in different temperature in Fig. 4, Table 3. Studies on incubation at physiological temperature (37°C) significantly accelerated the reduction process, producing a rapid color change and well-dispersed gold nanoparticles, demonstrating optimal reaction conditions. Higher temperatures, 48°C and 60°C, caused very fast reduction, but the excessive heat partially denatured the biomolecules in the shell extract, leading to aggregation, increased particle size, and decreased stability, as indicated by darker color changes [19].

Table 3: Effect of temperature of aqueous extract of AuNPs *Juglans regia*

Temperature	Nanometer
12ºc	546.0
24ºc	546.0
37ºc	546.0
48ºc	551.0
60ºc	557.2

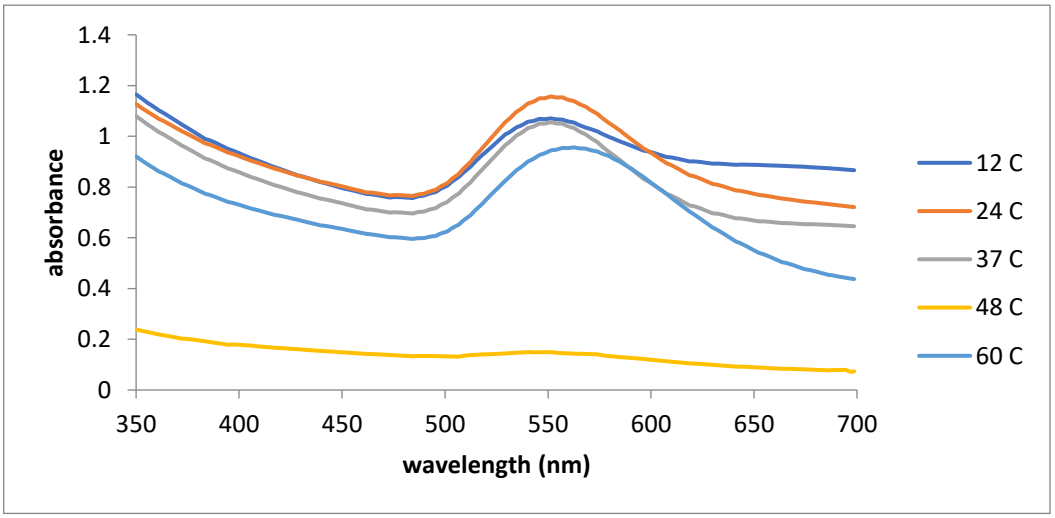

Fig. 4. Effect of temperature of AuNPs synthesized from aqueous extract of *J. regia*

Fourier transforms infrared (FTIR) spectroscopy

The interaction of gold nanoparticles with bio molecules of aqueous shell extract of *J. regia* was inferred by FTIR analysis showed a strong, broad peak recorded at 3266.70 cm-1due to O-H group stretching vibrations indicating the presence of phenol and alcohol. An absorption band appeared at 1636.64 cm-1corresponding to C=C stretching vibrations confirming the presence of alkenes aromatics is indicated by the C=C stretching vibrations between 1575 and 1675 cm-1 (Fig. 5). Similar study on the absorption band at 1636.64 cm^{-1} in your sample reflects C=C stretching vibrations, which confirms the presence of alkenes and aromatic compounds. In many biosynthesis studies, peaks in this region (approximately 1575–1675 cm^{-1}) are attributed to aromatic C=C or conjugated systems in flavonoids, terpenoids, and other phenolic constituents of plant extracts. These compounds not only contribute to reduction but also interact with growing AuNP surfaces through π-electrons or conjugated moieties, facilitating nanoparticle stabilization [20].

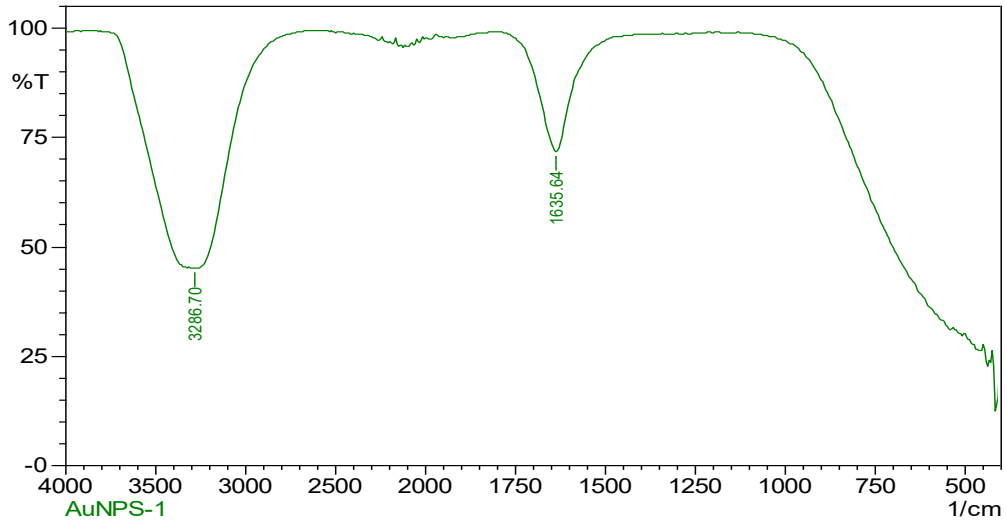

Fig. 5. FTIR analysis of AuNPs synthesized from *J. regia*

Energy dispersive X-ray spectroscopy (EDX)

EDX showed sharp peaks identical to elemental gold, confirming the presence of synthesized AuNPs which could be seen from the inset. The compositional analysis by EDX illustrated the purity of the gold, with spectra showing a strong AU single and NA signal from the grid on which the nanoparticles (Fig. 6). Typically, gold exhibits characteristic EDX peaks around 2.1 keV (Au Mα) and 9.7 keV (Au Lα), which are consistent with the observed spectrum. Such results validate the successful formation and elemental purity of AuNPs, in agreement with previous reports [21,22].

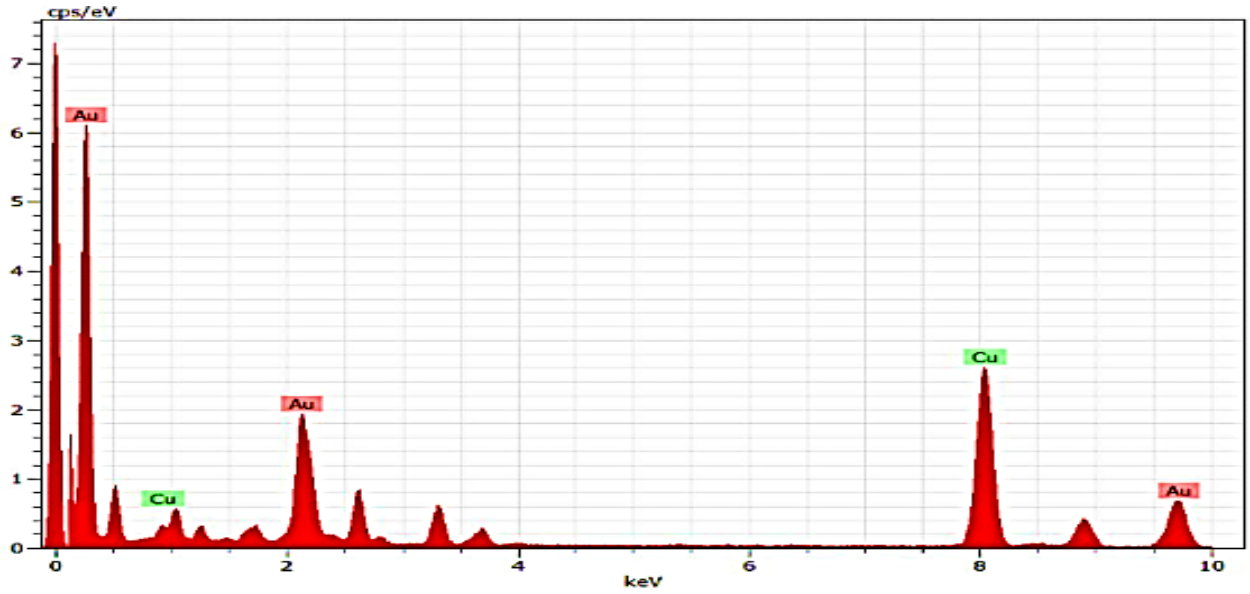

Fig. 6. EDAX analysis of AuNPs synthesized from aqueous extract of *J. regia*

X-ray diffraction (XRD)

The XRD pattern clearly indicated that the biosynthesized AuNPs are crystalline in nature. The strongest intensity of the diffraction peak of (111) lattice plane compared to the other peaks suggests its predominant orientation. The synthesis of gold nanoparticles showed characteristic diffraction peaks 38.21°, 44.39°, 64.62°, 77.59°, 81.75°, 98.16°, and 115.27° which is used for concluding the face-centered cubic (FCC) nature of gold nanoparticles (Fig. 7). These findings are consistent with standard data from the Joint Committee on Powder Diffraction Standards (JCPDS No. 04-0784) and confirm the successful formation of crystalline AuNPs. Moreover, the sharpness and intensity of the peaks imply good crystallite size and structural ordering, which are important factors influencing the optical and catalytic properties of gold nanoparticles [23].

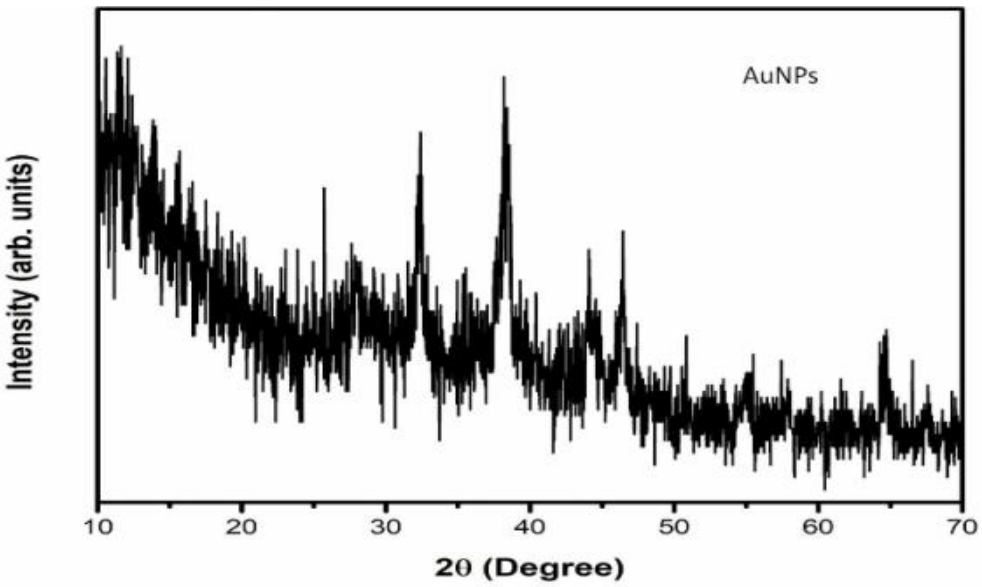

Fig. 7. XRD analysis of AuNPs synthesized from aqueous extract of *J. regia*

TEM Analysis

The AuNPs is well dispersed with *J. regia* extract surrounding it indicating the *J. regia* act as a capping agent to separate the AuNPs from aggregation. The average size of the AuNPs synthesized is mostly spherical in shape (Fig. 8). The absence of significant aggregation further confirms the efficiency of the *J. regia* extract in controlling nanoparticle growth and preventing particle–particle interaction. Such stabilization is crucial, as it preserves the nanoscale properties and improves the functional performance of AuNPs in biomedical and catalytic applications. Similar observations have been reported in green synthesis approaches, where plant extracts play a dual role as both reducing and capping agents [24,25].

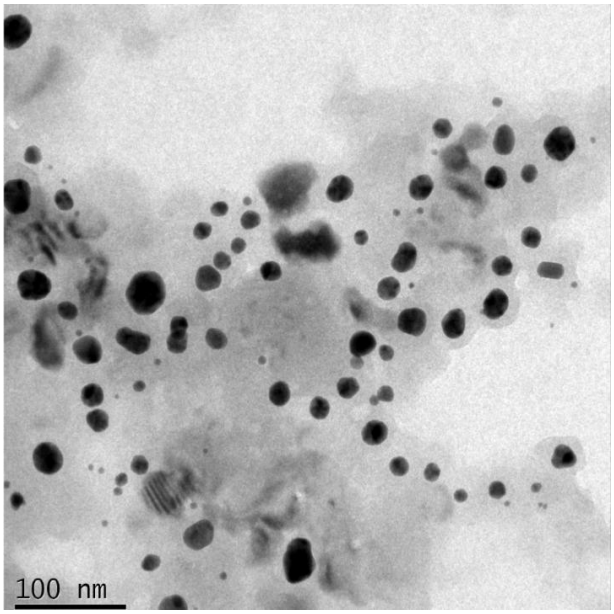

Fig.8. TEM analysis of AuNPs synthesized from aqueous extract of *J. regia*

Antioxidant activity – DPPH method

The dose-dependent activity of the sample with different concentrations from 100 – 500 µg/mL showed the chemical shift of the electrons produced to change the colour from purple to yellow which is shown in the table 4, Fig. 8. Sample concentration at 100 µg/mL showed 23.82 % of inhibition and at 500 µg/mL showed 46.36 % of inhibition (Fig. 9). According to the existing results obtained, the work showed good anti-oxidant potential from nanoparticles synthesized shell extract of *Juglans regia*. The moderate yet significant antioxidant activity suggests that the biosynthesized AuNPs possess promising free radical scavenging potential, comparable to previously reported plant-mediated nanoparticle systems. Such activity highlights their potential application in biomedical and pharmaceutical fields as natural antioxidant agents [26].

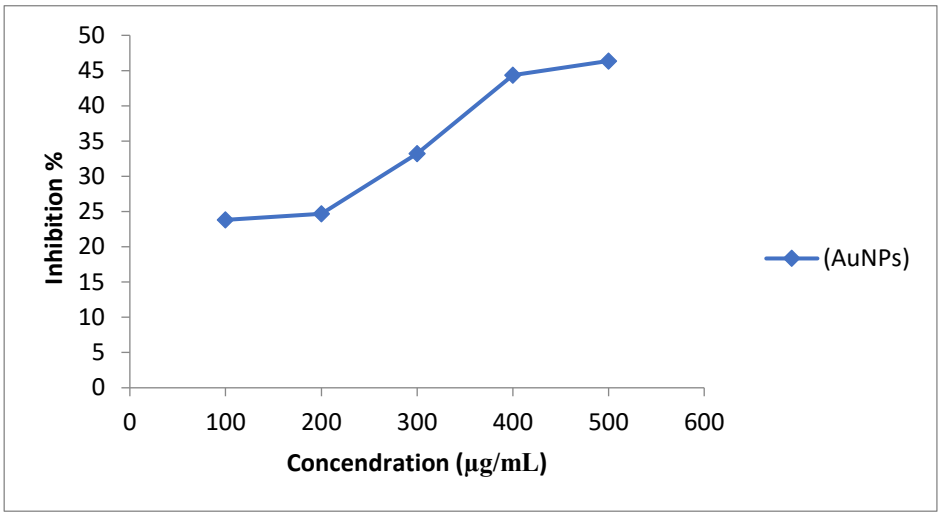

Fig.9. DPPH activity of AuNPs synthesized from aqueous extract of *J. regia*

Anti-cancer activity

The effect of AuNPs was examined on Vero cell line (normal cell) in terms of the effect of nanoparticles on cell proliferation by the MTT assay. The in vitro Cytotoxicity of the gold nanoparticles on MCF-7 cell lines showed that the increase in the concentration of AuNPs resulted in an increase in cell death. At 125 µg/ml concentration of the sample used showed 25.83% cell death and concluded that the nanoparticles they synthesized possess anticancer properties (Fig. 10,11). The presence of bioactive compounds from *Juglans regia*-extract on the nanoparticle surface may enhance therapeutic efficacy through synergistic effects. These findings are consistent with previous reports demonstrating that plant-mediated AuNPs exhibit selective toxicity toward cancer cells while maintaining minimal effects on normal cells, highlighting their promise for biomedical applications in cancer therapy [27].

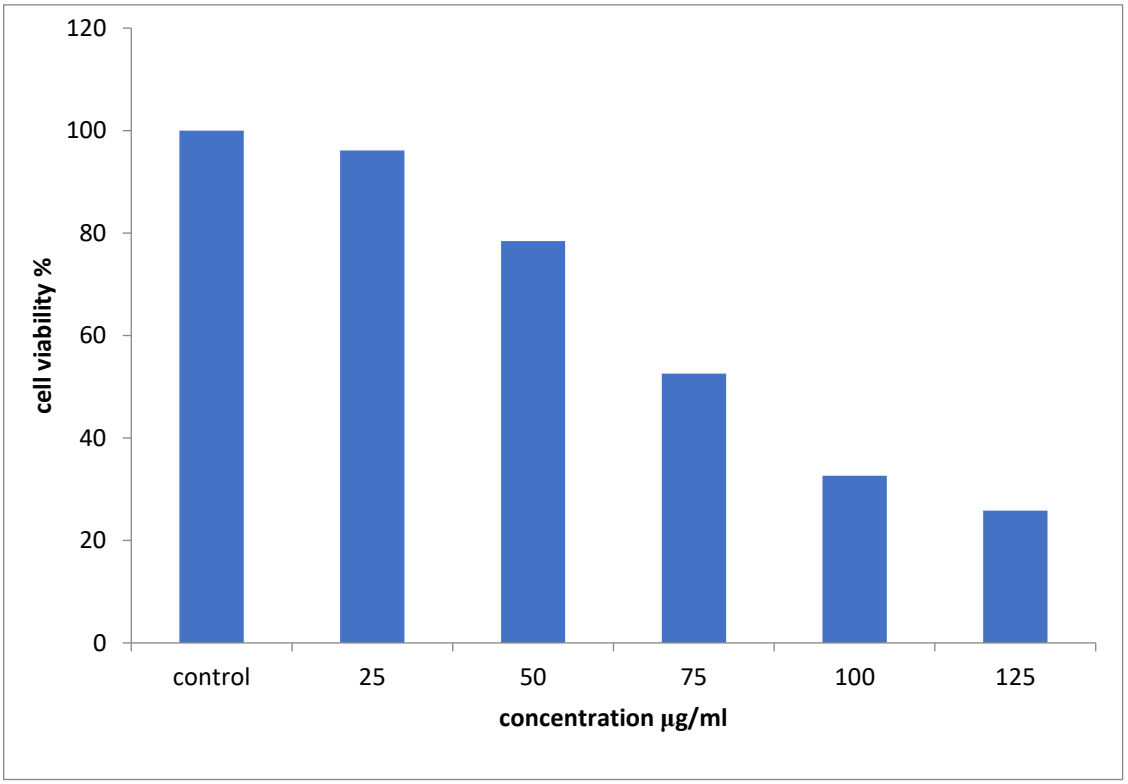

Fig. 10. Anticancer activity of AuNPs conjugates 5-FU against MCF-7 (Breast cancer cell)

Fig. 11

Anticancer activity of AuNPs conjugates 5-FU against MCF-7 (Breast cancer cell)

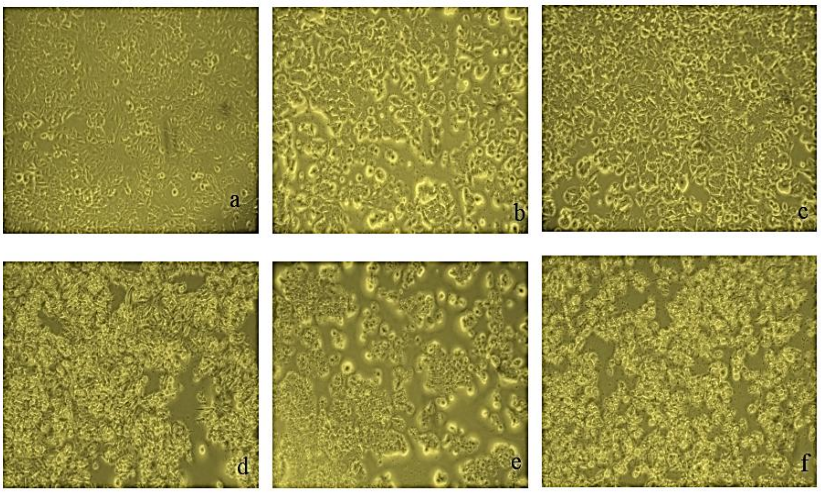

A- Control
B- cells treated 25µg/ml
C - cells treated 50µg/ml
D- cells treated 75µg/ml
E- cells treated 100µg/ml
F - cells treated 125µg/ml

AO/EB staining method

The control cells upon this staining, in this study; exhibit only such green structures which imply that they are healthy and not affected by the gold nanoparticles. There was no significant apoptosis detected in the control cells whereas the AuNPs treated MCF-7 cells resulted in morphological apoptotic changes. The cells treated with AuNPs exhibited early apoptosis, and late apoptotic cells having bright green patches of cells with intact membrane and green nuclei representing their perinuclear chromatin condensation, asymmetrically localized light orange crescent nuclei with increased volume and dark orange. Fluorescence depicting their chromatin in either fragmented or condensed form. In the early apoptotic stage, bright green patches of cells with intact membrane and green nuclei representing their perinuclear chromatin condensation were detected. Hence, in this study the images of AO/EB staining of the cancer cell lines confirms necrotic cell death as there is presence in the apoptosis cell as earlier and later (Fig. 12). These findings confirm that AuNP treatment induces apoptosis in cancer cells, likely through mechanisms such as reactive oxygen species (ROS) generation, mitochondrial dysfunction, and activation of intrinsic apoptotic pathways. The clear distinction between healthy control cells and apoptotic treated cells highlights the selective cytotoxic potential of AuNPs. Such observations are consistent with earlier studies reporting nanoparticle-induced apoptosis in cancer cells, supporting their potential application in anticancer therapy [28].

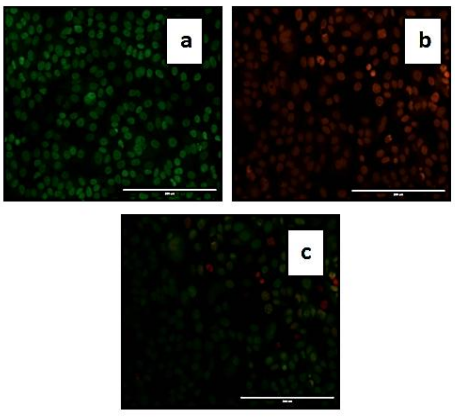

A- Control cells
B- Cells treated with AuNPs synthesized *J. regia* aqueous extract (IC50 – 79.15 µg/ml)
C- Early apoptotic cells treated with AuNPs synthesized *J. regia* aqueous extract (IC50 – 79.15 µg/ml)

Fig. 12. AO/EB Staining

CONCLUSION

In conclusion, the present study demonstrated the successful green synthesis of gold nanoparticles (AuNPs) using the aqueous extract of *Juglans regia*, which acted as both a reducing and capping agent. The formation of AuNPs was confirmed through various characterization techniques, including UV–Vis spectroscopy, EDX and XRD analysis, which

revealed their crystalline nature and high purity with a face-centered cubic (FCC) structure. Overall, the findings highlight that *Juglans regia*-mediated AuNPs possess promising antioxidant and anticancer properties, suggesting their potential application in biomedical and pharmaceutical fields.

REFERENCES

1. Iravani, S. (2011). Green synthesis of metal nanoparticles using plants. Green Chemistry, 13, 2638–2650.
2. Ahmed, S., Ahmad, M., Swami, B. L., & Ikram, S. (2016). A review on plants extract mediated synthesis of silver nanoparticles for antimicrobial applications. Journal of Advanced Research, 7(1), 17–28.
3. Mittal, A. K., Chisti, Y., & Banerjee, U. C. (2013). Synthesis of metallic nanoparticles using plant extracts. Biotechnology Advances, 31(2), 346–356.
4. Singh, P., Kim, Y. J., Zhang, D., & Yang, D. C. (2016). Biological synthesis of nanoparticles from plants and microorganisms. Trends in Biotechnology, 34(7), 588–599.
5. Gurunathan, S., et al. (2014). Cytotoxicity and apoptotic effect of silver nanoparticles in human cancer cells. International Journal of Nanomedicine, 9, 5885–5896.
6. Dhanalakshmi, T.; Rajendran, S. 2012. Synthesis of silver nanoparticles using Tridax procumbens and its antimicrobial activity. Arch. Appl. Sci. Res., 4: 1289–1293.
7. O. O. Debiyi and F. A. Sofowora. 1978. Pytochemical screening of medical plants," Iloyidia, vol. 3, pp. 234–246.
8. G. E. Trease and W. C. Evans. 1989. Phenols and phenolic glycosides," in Textbook of Pharmacognosy, vol. 12, pp. 343–383, Balliese, Tindall and Co Publishers, London, UK.
9. T. S. Roopashree, R. Dang, R. H. S. Rani, and C. Narendra. 2008. Antibacterial activity of antipsoriatic herbs: Cassia tora, Momordica charantia and Calendula officinalis," International Journal Applied Research in Natural Products, vol. 1, no. 3, pp.20–28.
10. M. R. Szabo, C. Idiţoiu, D. Chambre, and A. X. Lupea. 2007. Improved DPPH determination for antioxidant activity spectrophotometric assay. Chemical Papers, 61(3): 214–216.
11. T. Mossmann. 2012. Rapid colorimetric assay for cellular growth and survival: application to proliferation and cytotoxicity assays, J. Immunol. Methods. 55–63.
12. Leeba Balan, Sriram Chandrasekaran, Mani Gajendiran, Raaman Nanjian. 2021. Synthesis of silver nanoparticles from Pedalium murex L. and its antiproliferative activity against breast cancer (MCF-7) cells. Journal of Molecular Structure., 1242: 130695.
13. Jamil, Y.M.S.; Al-Hakimi, A.N.; Al-Maydama, H.M.A.; Almahwiti, G.Y.; Qasem, A.; Saleh, S.M. Optimum Green Synthesis, Characterization, and Antibacterial Activity of Silver Nanoparticles Prepared from an Extract of Aloe fleurentinorum. Int. J. Chem. Eng. 2024, 2024, 2804165.
14. Pereira, J. A., et al. (2007). Phenolic compounds and antimicrobial activity of walnut (*Juglans regia*-L.) leaves, green husks and fruits. Food and Chemical Toxicology.
15. Oliveira, I., et al. (2008). Walnut (*Juglans regia*-L.) leaves: chemical composition, antioxidant activity and antimicrobial potential. Food and Chemical Toxicology.
16. Edeoga, H. O., et al. (2005). Phytochemical constituents of some Nigerian medicinal plants. African Journal of Biotechnology.
17. Aljabali et al. (2018) – Discussion on SPR and color change in green AuNP synthesis, typical peaks ~527–535 nm. Nanomaterials, 8(3):174, pp. 3–4.
18. Priya, M.R.K., Iyer, P.R. Biosynthesis and optimization of highly stable gold nanoparticles, nanoconjugates, nanodrug conjugates and chitosan nanoconjugates using medicinal plants. Bull Natl Res Cent 46, 134 (2022).
19. Song, J. Y., & Kim, B. S., 2009. Rapid biological synthesis of gold nanoparticles using plant leaf extracts. Bioprocess and Biosystems Engineering, 32: 79–84.
20. Dauthal, P., Mukhopadhyay, M. Phyto-synthesis and structural characterization of catalytically active gold nanoparticles biosynthesized using Delonix regia leaf extract. 3 Biotech 6, 118 (2016).
21. Khan, Z., et al. (2013). Synthesis and characterization of gold nanoparticles using plant extracts. Colloids and Surfaces B: Biointerfaces, 102, 578–584.
22. Amendola, V., & Meneghetti, M. (2009). Size evaluation of gold nanoparticles by UV–vis spectroscopy. Journal of Physical Chemistry C, 113(11), 4277–4285.
23. Philip, D. (2010). Green synthesis of gold and silver nanoparticles using Hibiscus rosa sinensis. Physica E: Low-dimensional Systems and Nanostructures, 42(5), 1417–1424.
24. Mittal, A. K., Chisti, Y., & Banerjee, U. C. (2013). Synthesis of metallic nanoparticles using plant extracts. Biotechnology Advances, 31(2), 346–356.
25. Ahmed, S., Ahmad, M., Swami, B. L., & Ikram, S. (2016). A review on plants extract mediated synthesis of silver nanoparticles. Journal of Advanced Research, 7(1), 17–28.
26. Iravani, S. (2011). Green synthesis of metal nanoparticles using plants. Green Chemistry, 13, 2638–2650.
27. Mosmann, T. (1983). Rapid colorimetric assay for cellular growth and survival: Application to proliferation and cytotoxicity assays. Journal of Immunological Methods, 65(1–2), 55–63.
28. Dykman, L., & Khlebtsov, N. (2012). Gold nanoparticles in biomedical applications. Chemical Society Reviews, 41(6), 2256–2282.